Structure and Properties of Some Layered U_2O_5 phases: a Density Functional Theory Study

Marco Molinari,[a,b] *Nicholas A. Brincat,*[a,c] *Geoffrey C. Allen,*[c,d] *Stephen C. Parker*[a,*]

[a]Department of Chemistry, University of Bath, Claverton Down, Bath, BA2 7AY, UK

[b]Department of Chemistry, University of Huddersfield, Queensgate, Huddersfield, HD1 3DH, UK

[c]AWE plc, Aldermaston, Reading, UK, RG7 4PR

[d]Interface Analysis Center, University of Bristol, Bristol, UK.

ABSTRACT. U_2O_5 is the boundary composition between the fluorite and layered structures of the $UO_{2\rightarrow3}$ system and the least studied oxide in the group. δ-U_2O_5 is the only layered structure proposed so far experimentally, although evidence of fluorite-based phases has also been reported. Our DFT work explores possible structures of U_2O_5 stoichiometry by starting from existing M_2O_5 structures (where M is an actinide or transition metal) and replacing the M ions with uranium ions. For all structures, we have predicted structural and electronic properties including bulk moduli and band gaps. The majority of structures were found to be less stable than δ-U_2O_5. U_2O_5 in the R-Nb_2O_5 structure was found to be a competitive structure in term of stability whereas U_2O_5 in the Np_2O_5 structure was found to be the most stable overall. Indeed, by including the vibrational contribution to the free-energy using the frequencies obtained from the optimized unit cells we predict that Np_2O_5 structured U_2O_5 is the most thermodynamically stable under ambient conditions. δ-U_2O_5 only becomes more stable at high temperatures and/or pressures. This suggests that a low temperature synthesis route should tested and so potentially opens a new avenue of research for pentavalent uranium oxides.

KEYWORDS. U_2O_5, pentavalent uranium oxide, diuranium pentoxide, oxidised UO_2, layered uranium oxide, ab initio calculation, thermodynamic properties.

Introduction

U_2O_5 marks an important, yet underexplored, area of the uranium-oxygen phase diagram. Although its' practical applications have received little attention, owing to its instability relative to both higher and lower oxides [1-8]. One of its intriguing features is that it represents the composition of the transition point between the fluorite and layered uranium oxides, with reports of it forming in both types of structure [1, 9]. As the existing data in the literature concerning any of the reported U_2O_5 polymorphs is extremely limited, again most likely due to difficulties in synthesising it, computational investigations provide a convenient means of exploring the structural and electronic properties of this material and relating them to the coordination environments of uranium.

The only reported study of fluorite U_2O_5 is from Hoekstra *et al.*, who give details on the synthesis and structures of α-, β- and γ-U_2O_5 (although not enough information is available to produce a full atom description) [1]. α-U_2O_5 was prepared by heating a mixture of UO_2 and U_3O_8 (673 K at 30 kbar) and found to have a density of 10.5 gcm^{-3}, approximately 0.7 gcm^{-3} less than other fluorite based phases, which suggests that the structure might be slightly closer to a layered type oxide [10, 11]. β-U_2O_5 and γ-U_2O_5 were prepared by heating the same mixture in excess of 1073 K at 40-50 kbar and 60 kbar respectively. β-U_2O_5 has a hexagonal cell with a=b=3.813 Å and c=13.180 Å with a density of 11.15 gcm^{-3}, whereas γ-U_2O_5 has a monoclinic cell with a=5.410, b=5.481, c=5.410 Å and β=90.49° with a density of 11.36 gcm^{-3}. These densities suggest that it is more likely to be a defective fluorite UO_2 [12, 13]. The lack of any atomic coordinates for fluorite based U_2O_5 structures means that UO_2 supercells with additional oxygen interstitials (Oi) are required to investigate these types of structure quantum mechanically [12, 13].

The only full crystallographic structure reported in the literature is the layered δ-U_2O_5 polymorph. It has a density of 8.22 gcm^{-3} and crystallises in the orthorhombic *Pnma* space group with a= 6.849, b=8.274 and c=31.706 Å [9]. It contains a mixture of six-fold (distorted octahedral) and seven-fold (distorted pentagonal bipyramidal) uranium environments and the structure is similar to U_3O_8,

essentially an oxygen deficient version of this higher oxide. No thermodynamic information has been gathered experimentally for U_2O_5, nor has there been any further structural investigation since the original experiments of Hoekstra [1 9]. Early XPS studies have suggested a mixture of U^{4+} and U^{6+} ions [14], but more recent experiments have proposed U_2O_5 is composed entirely of U^{5+} ions [15]. Brincat *et al.* showed that the DFT + U methodology was able to reproduce the structure of δ-U_2O_5 [3] while Andersson *et al.* reported it to be thermodynamically unstable (with respect to U_3O_8) with the highest formation energy of any uranium oxide [4]. Our aim is to develop reliable structural models to aid in the identification of possible phases and give a quantitative description of their relative stability.

Methodology

Calculations were performed using the Vienna *Ab Initio* Simulation Package (VASP) [16, 17], with the PBE [18] exchange-correlation functional within the generalised gradient approximation (GGA). The Dudarev approach [19] to the GGA + U methodology [20] was employed to enforce localisation of U 5*f* electrons. We have used an effective U_{eff} (*U-J*) parameter of 3.96 eV. The values of the *U* and *J* parameters were 4.5 eV and 0.54 eV respectively, which were taken from the XPS experiments of Yamazaki and Kotani on UO_2 [21]. No such parameters have been derived for U_2O_5 (or any other uranium oxides) and so in the interest of transferability of results we have used these values, as in our previous works [3, 10]. Work in the literature has demonstrated that changing the effective *U* parameter mainly affects the predicted band gap, and has considerably less impact on the other calculated properties [22].

Spin-orbit coupling has not been included in any of the calculations described here as it has been previously demonstrated on actinide dioxides [23, 24] and U_3O_8 [25] that the effects on structural and electronic properties and relative stabilities are inconsequential. The structural optimisations presented here were all allowed to proceed with unconstrained symmetries so that all volume and internal structure parameters were relaxed. The total energy was converged to at least 1 x 10^{-6}

eV/atom for the electronic relaxation and the ionic relaxation was performed until the Hellmann-Feynman forces on each atom were less than 0.01 eVÅ^{-1}.

Convergence of the energy was reached with a cutoff energy of 500 eV to remove errors due to Pulay stress [26] during cell relaxation and automatically generated *Γ*-centred Monkhorst-Pack *k*-meshes of *δ*-U_2O_5 3 x 2 x 1, Np_2O_5 4 x 6 x 4, *R*-Nb_2O_5 6 x 6 x 4, *Z*-Nb_2O_5 6 x 6 x 6, *N*-Nb_2O_5 1 x 4 x 2, B-Ta_2O_5 4 x 6 x 6, *α*-V_2O_5 2 x 6 x 2 and *β*-V_2O_5 3 x 6 x 4. Although this results in a range of *k*-mesh densities convergence was reached in each case. All structures are free of imaginary modes. Vibrational frequencies are presented in Figure S1-S8. Elastic constants and bulk moduli were calculated for all polymorphs as detailed in our previous work on UO_3 [10].

Ferromagnetic ordering was used for all of the M_2O_5 structures, as the difference in energy between ferromagnetic and antiferromagnetic orderings was found to be negligible for *δ*-U_2O_5 [3].

Results and Discussion

We have simulated different structures with U_2O_5 composition; before assessing their order of stability, here we describe their structures.

Structural properties. A number of alternative M_2O_5 (where M is an actinide or transition metal) structures have been investigated, replacing the metal ion with uranium, including Np_2O_5 [27], Nb_2O_5 [28-30], Ta_2O_5 [31], and V_2O_5 [32, 33] polymorphs. All relaxed structures retain the coordination environments of the original M_2O_5 systems, although the symmetry is often lowered. This may be a direct consequence of the strain imposed by the large uranium cation (0.84 Å) substituting the transition metal ions (V, Nb, Ta) which are significantly smaller (0.54, 0.69 and 0.69 Å respectively) [34]. As the lattice parameter of the original structures cannot be directly compared to our simulation results, we do not report their details. We only report the experimental structure of Np_2O_5 as a comparison to our calculated structure of U_2O_5 in the Np_2O_5 structure. From the comparison between the experimental and the calculated lattice parameters (Table 1) the agreement is excellent, most likely due to the

similarity between uranium and neptunium atomic radii (0.84 and 0.75 Å respectively[34]). If the change in volume is ascribed to the extra space filling of spherical uranium ions, the increase in volume would be predicted to be 5.7 Å^3, which is close to the increase of 5 Å^3 actually calculated. To note, as customary with the PBE + U, the cell volume is overestimated for both U_2O_5 and Np_2O_5, compared to the experimental data. Structural properties of the various systems are collated in Table 1 and Table 2 whilst their relaxed structures are shown in Figure 1 to Figure 4. All structures are presented in SI.

***δ*-U_2O_5**. The simulated unit cell contains only U^{5+}, half in pentagonal bipyramidal and half in octahedral coordination (Fig. 1a) environments. This coordination is equivalent to the one in the experimental unit cell. The layers stack in an eclipsed fashion such that the coordination of a given uranium ion is identical to the one directly above or below. The structure [9] resembles oxygen deficient *α*-U_3O_8. The U-Oax bonds (Oax are oxygen atoms lying above and below the equatorial plane of the coordination environment) between the layers range between 2.105 and 2.107 Å (longer than a typical uranyl bond [10 35]) and equatorial bonds similar to those in U_3O_8[3].

U_2O_5 in Np_2O_5 structure. The simulated structure consists of 8 uranium environments[27], 4 with pentagonal bipyramidal coordination (although 2 U-Oeq bonds are longer than 2.6 Å, Oeq are oxygen atoms lying in the equatorial plane of the coordination environment) and 4 with octahedral coordination (Fig. 1b). Each pentagonal bipyramidal U site contains one U-Oax bond ~1.97 Å, slightly longer than a uranyl ion bond (1.7 – 1.9 Å). All uranium ions are predicted to be U^{5+}. The stacking of layers gives alternating octahedral and pentagonal bipyramidal coordination, which is similar to *β*-U_3O_8 [3].

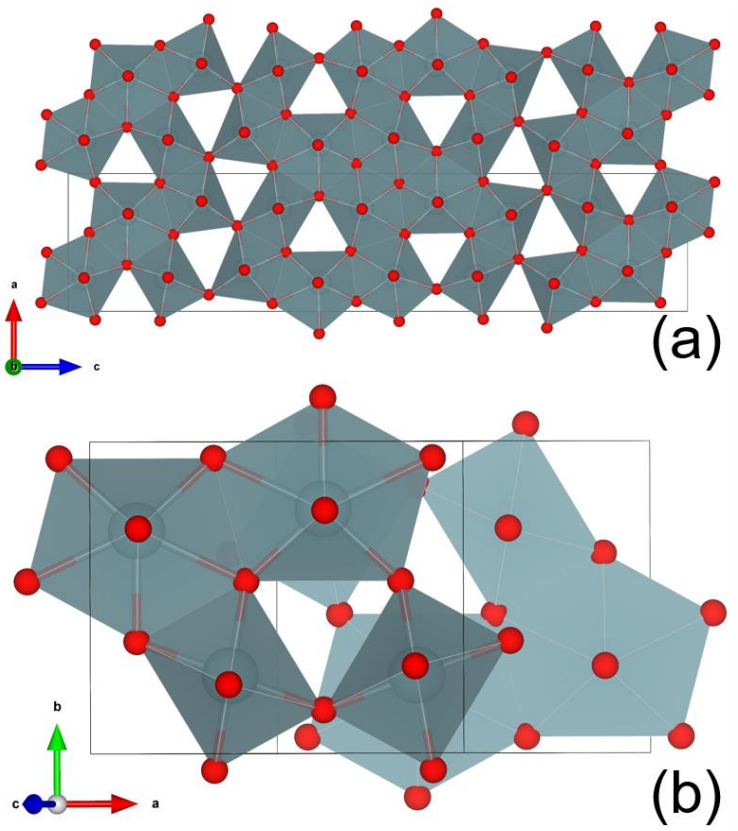

Figure 1. Simulated structure of the (a) top view of δ-U_2O_5 and (b) top view of U_2O_5 in the Np_2O_5 structure.

Table 1. Predicted properties of U_2O_5. Space groups are calculated to a tolerance of 0.01 Å. Δ% is the percentage difference between a calculated structure and experiment and is not presented for any of the M_2O_5 structures (where M is a metal ion other than uranium). The enthalpy of formation (E_{form}=E(U_2O_5) – 2E(U) – 5E(O)) is calculated with respect to the energy of α-U metal (8.43 eV/U) and the O_2 molecule (-4.93 eV/O ca. expt. -5.10 eV/O [36]). The energy of an O atom was predicted to be −4.93 eV, calculated from an O_2 molecule in a 20 Å box using the Γ-point. * The experimental structure is for Np_2O_5.

Phase	**Method**	**Lattice Parameters (Å)**			**Lattice Parameters (°)**			**Vol** ($Å^3/U_2O_5$)	**Space Group**	**E_{gap}** (eV)	**B** (GPa)	**E_{form}** (eV/U_2O_5)
		a (Δ%)	***b*** (Δ%)	***c*** (Δ%)	***α*** (Δ%)	***β*** (Δ%)	***γ*** (Δ%)					
***δ*-U_2O_5** [9]	Expt.	6.85	8.27	31.71	90.0	90.0	90.0	112.27	*Pnma (62)*	-	-	-
	PBE + U	7.0225 (2.52)	8.4219 (1.84)	31.4605 (-0.79)	90.0	90.0	90.0	116.29 (3.58)	*Pcma (55)*	1.69	160	-23.01
Np_2O_5 [27]	Expt.*	8.17	6.58	9.31	90.0	116.1	90.0	112.46	*P2/c (13)*	-	-	-
	PBE + U	8.1358 (-0.42)	6.8289 (3.78)	9.3972 (0.94)	90.00	115.91 (-0.16)	90.00	117.41 (4.40)	*I2/a (15)*	2.45	133	-23.24
R-Nb_2O_5 [28]	PBE + U	4.2126	4.3586	14.9779	106.82	90.00	89.99	131.63	*Pm (6)*	2.07	149	-22.98
Z-Nb_2O_5 [29]	PBE + U	7.0092	5.2237	5.8121	89.97	104.67	90.04	108.40	*P1 (1)*	2.20	88	-22.45
N-Nb_2O_5 [30]	PBE + U	31.4749	4.2998	19.1689	90.05	124.94	89.90	132.91	*P1 (1)*	1.30	108	-22.48
B-Ta_2O_5 [31]	PBE + U [+]	14.2946	5.2982	6.1399	90.00	104.40	90.01	112.60	*P-1 (2)*	2.25	57	-22.72
***α*-V_2O_5** [32]	PBE + U	11.5425	4.3638	10.5977	90.02	90.00	89.98	133.45	*$P2_1$ (4)*	1.99	82	-22.35
***β*-V_2O_5** [33]	PBE + U	6.6125	4.0259	7.3203	90.00	79.71	90.00	95.87	*Pm (6)*	1.35	176	-21.94

Table 2. Coordination and charges of Uranium in simulated U_2O_5 phases.

	Number of U Environments per simulated unit cell							
U environment	**δ-U_2O_5**	**Np_2O_5**	**R-Nb_2O_5**	**Z-Nb_2O_5**	**N-Nb_2O_5**	**B-Ta_2O_5**	**α-V_2O_5**	**β-V_2O_5**
U^{5+} trigonal bipyramid								
U^{5+} distorted octahedron	8		4	4		8	8	
U^{5+} octahedron	8	4			16			
U^{5+} pentagonal bipyramid	16	4						
U^{5+} 7-fold								2
U^{6+} octahedron					8			
U^{6+} 7-fold								1
U^{4+} distorted octahedron					8			
U^{4+} 7-fold								1
Uranyl Bond		U^{5+}-O 1.98Å*			U^{6+}-O 1.97Å			U^{6+}-O 1.93Å

U_2O_5 in Nb_2O_5 structure. We have simulated R-[28] Z-[29] and N-[30] Nb_2O_5 polymorphs. It is worth commenting that R- and N-Nb_2O_5 phases are anatase-like structures, and as shown in Figure 2a and Figure 2b respectively, have layers of edge sharing MO_6 octahedra. In R-Nb_2O_5 the layers are continuous in the c direction (Figure 2a), while in N-Nb_2O_5 they are separated by 2 layers of a skutterudite-like structure resembling δ-UO_3. The structure can be considered as a Magneli-like structure [37], which has alternating MO_6 rich layers perovskite (without the A cation, i.e. ReO_3 structured) layers. Z-Nb_2O_5 does not resemble the anatase structure and is more comparable to a distorted brookite structure (Figure 2c). All systems have monoclinic symmetry. In the R- and Z-Nb_2O_5 phases all uranium ions are U^{5+} in octahedral coordination. In contrast, for the N-Nb_2O_5 structure we found a mixture of U^{4+} (25%), U^{6+} (25%) and U^{5+} (50%), again all uranium ions are in octahedral coordination. However, U^{4+} sites have a highly distorted octahedral environment whereas U^{6+} have the least distorted octahedral environment with a U-Oax bond of 1.97 Å.

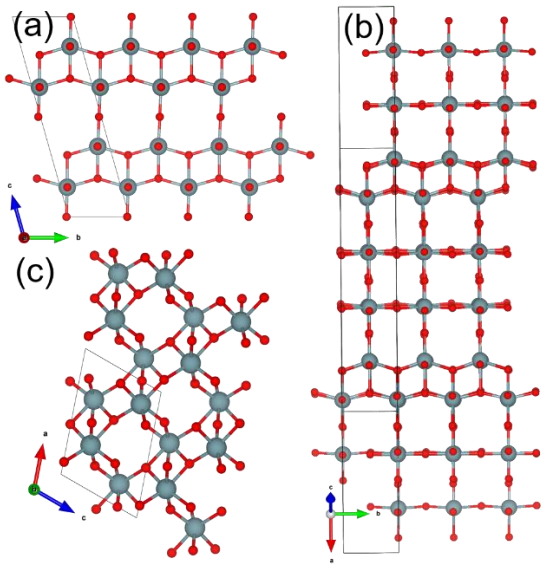

Figure 2. U_2O_5 in (a) R-Nb_2O_5, (b) N-Nb_2O_5, and (c) Z-Nb_2O_5 structures.

U_2O_5 in Ta_2O_5 structure. Although many polymorphs exist for this oxide, they are for the most part very similar to Nb_2O_5. Thus, only one polymorph was simulated (B-Ta_2O_5) [31]. All uranium ions are in distorted octahedral coordination and predicted to be U^{5+}.

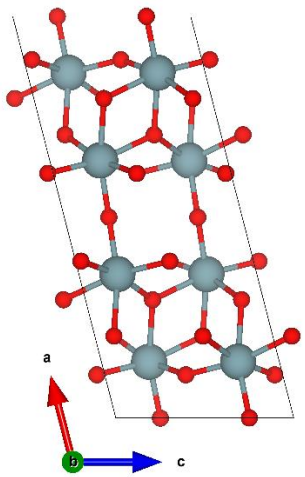

Figure 3. U_2O_5 in the B-Ta_2O_5 structure.

U_2O_5 in V_2O_5 structure. Two polymorphs have been studied, α- and β-V_2O_5. The α- polymorph crystallises in an orthorhombic unit cell, with all uranium ions in distorted octahedral environments [32]. β-V_2O_5 has U sites in 7-fold coordination [33], with the equatorial bonds extended above and below the equatorial plane in a similar manner to α-UO_3 [10]. U sites are occupied entirely by U^{5+} in α-V_2O_5 whereas the distribution is 25% U^{4+}, 25% U^{6+} and 50% U^{5+} in β-V_2O_5. U^{6+} sites have U-O axial bonds of 1.93 Å.

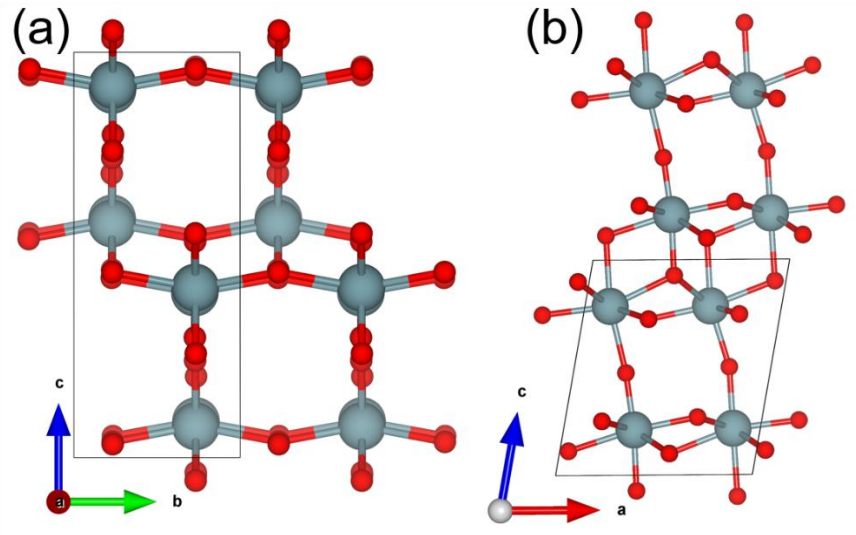

Figure 4. U_2O_5 in the (a) α- and (b) β-V_2O_5 structures.

Stability. The formation energies of the simulated structures with U_2O_5 composition are listed in Table 1. For clarity, we have plotted these energies against the volume per U_2O_5 unit in Figure 5. There is a clear dependence of the formation energy on the volume, with a decrease in stability for volumes smaller or larger than the most stable phases (Np_2O_5 and U_2O_5).

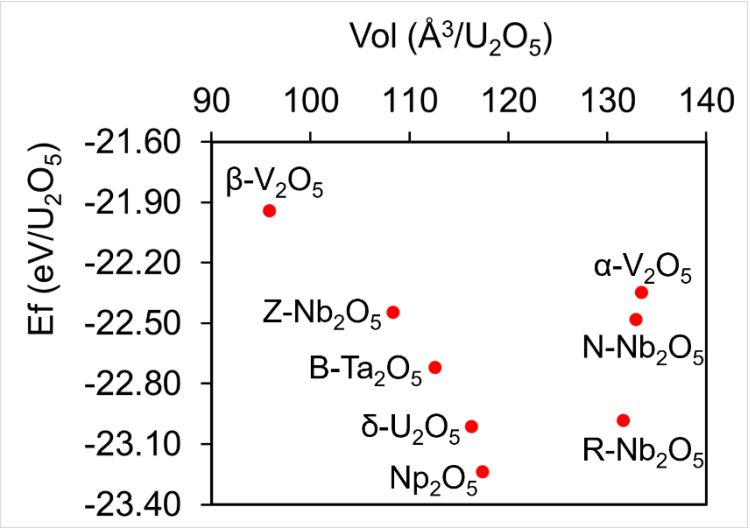

Figure 5. Stability plot of formation energy per U_2O_5 in eV vs volume per U_2O_5 unit. The phases are named with the original M_2O_5 structures for clarity.

There are a number of factors, including the distribution of uranium charges and uranium coordination that influence the stability. The Np_2O_5 structure is the most stable overall, 0.23 eV more stable than δ-U_2O_5 although both structures contain half U in pentagonal bipyramidal and half in octahedral coordination. As with δ-U_2O_5, the Np_2O_5 structure resembles oxygen deficient U_3O_8. R-Nb_2O_5 is found to be just slightly less stable than δ-U_2O_5 (0.03eV). In this structure U ions are all U^{5+} and all in distorted octahedral coordination. Phases with mixed U charges are amongst the most unstable although this effect is exacerbated by small volumes.

The other phases follow the order of stability of Np > Nb/Ta > V, with the Np_2O_5 structure noticeably more stable than δ-U_2O_5. As U^{5+} prefers higher coordination numbers compared to the 6-fold octahedral coordination, all the structures featuring uranium ions entirely in six-fold coordination are consequently less stable. V_2O_5 structured oxides are the least stable with the β- polymorph less stable than the α-V_2O_5 structure, due to the presence of U in mixed oxidation states (U^{4+} and U^{6+}) compared to α-V_2O_5 comprised of only U^{5+} ions.

These energetics show that U_2O_5 could crystallise in the Np_2O_5 structure, but due to the relative instability of the U_2O_5 stoichiometry compared to the other uranium oxides, it has not been synthesised or reported experimentally. The difficulty in synthesising layered U_2O_5 is likely to stem from the fact that the structure is essentially oxygen deficient U_3O_8 and U^{5+} is more stable in pentagonal bipyramidal coordination [3]. This relative instability of δ-U_2O_5 (and (Np) U_2O_5) likely arises from the presence of octahedrally coordinated uranium ions, it is highly favourable for this polymorph to gain more oxygen so that U^{6+} can occupy octahedral sites and U^{5+} may retain pentagonal bipyramidal coordination. This coordination behaviour is observed for both α- and β-U_3O_8 phases [3].

One can also consider the formation of the studied U_2O_5 phases as a function of pressure representing a range of conditions; from negative pressure (high temperature) to positive (high) pressure. The formation enthalpies as a function of pressure are presented in Figure S9 and are normalised with respect to the most stable U_2O_5 (i.e. the Np_2O_5 structure) such that $\delta H_f = \Delta H(x) - \Delta H(Np_2O_5)$, where x is the phase in question and $\Delta H(x)$ correspond to Eform in Table 1. Of interesting note is that we predicted that at high pressure (above 97 kbar) U_2O_5 will be more thermodynamically stable in β–V_2O_5 structure, although its dynamical stability will need to be checked via the calculation of the vibrational frequencies.

Using the predicted vibrational frequencies (Figure S1 to S8) calculated for each unit cell, we evaluated the vibrational contribution to a number of thermodynamic properties such as the Helmholtz free energy A_{vib} (Figure S10), vibrational entropy S_{vib} (Figure S11) and vibrational energy E_{vib} (Figure S12), Helmholtz free energy $A_{tot} = E_{form} + A_{vib}$ (Figure S13) and the zero point energy (ZPE, Table 3). All these properties are expressed per U_2O_5 unit and a sample of values at 300 K is presented in Table 3. A full calculation of the phase stability for U_2O_5 phases is beyond the scope of this work, however, the calculations show that the energy minimised δ-U_2O_5 phase has a lower vibrational entropy and a smaller ZPE than the Np_2O_5 phase. Hence, at high temperatures the δ-U_2O_5

phase will be thermodynamically favoured. Using our calculated values δ-U_2O_5 is predicted to be the preferred structure at around 800 C and 0 bar (Figure S13). Furthermore, the delta phase has a smaller molar volume, which means that it is further stabilised at high pressures, where the PV term in the Gibbs free energy will dominate. Thus it is not surprising that given the synthesis conditions reported for U_2O_5,[1, 9] i.e. high temperatures and pressures that our predicted Np_2O_5 phase has not been spotted.

Table 3. Predicted thermodynamic properties of U_2O_5 phases at 300 K using the zone centre vibrational frequencies.

Phase	A_{vib} (meV)	S_{vib} (meV/K)	E_{vib} (meV)	ZPE (meV)	A_{tot} (eV)
Np_2O_5	156	1.61	638	380	-23.08
δ-U_2O_5	112	1.79	647	371	-22.90
B-Ta_2O_5	205	1.46	643	401	-22.52
β-V_2O_5	231	1.33	630	407	-21.71
Z-Nb_2O_5	154	1.5	606	358	-22.29
R-Nb_2O_5	89	1.72	604	346	-22.89
α-V_2O_5	214	1.46	653	414	-22.14
N-Nb_2O_5	70	1.92	645	360	-22.41

Elastic properties. It is somewhat complicated to compare elastic constants, which are presented in Table S1. Thus we will focus on the bulk modulus for the different structures. There is no evident

correlation between the bulk moduli and the volume or formation energy of the U_2O_5 phases. The only noticeable correlation is that those structures with mixed charges (U^{6+} and U^{4+}) have higher bulk modulus (β-V_2O_5 and N-Nb_2O_5). However, as these structures are amongst the least stable, they are unlikely to be readily synthesised.

Electronic properties. The experimental electronic properties of U_2O_5 are not currently available and the only simulated electronic properties of δ-U_2O_5 are that of Brincat *et al*. [3]. In keeping with the higher layered oxides U_3O_8 [3] and UO_3 [10], all structures are predicted to be charge transfer insulators, with a conductance band composed of U 5f states and valence band comprised of O 2p states, with higher energy U 5f states at the core. The presence of U 5f states in the valence band suggests a degree of covalent mixing with O 2p (fully ionic bonding would feature no overlapping states). There is very little overall contribution from U 6d states, with most of it confined to the lower valence band. There is a great variation in predicted band gaps, with δ-U_2O_5 predicted to be 1.69 eV, which is relatively close to the experimentally determined α-U_3O_8 band gap of 1.76 eV [38]. Those structures with mixed charges (U^{6+} and U^{4+}) have lower band gaps (β-V_2O_5 and N-Nb_2O_5), whereas all other structures have band gaps in line with PBE + U U_3O_8 (2.05 – 2.23 eV) [3].

Conclusions

Our results show clearly that U_2O_5 structures prefer U ions in homogeneous U^{5+} oxidation states rather than a mixed charge state (U^{4+} and U^{6+}) and that higher coordination numbers are favoured, such as pentagonal bipyramids compared to octahedra. The simulations predict that the Np_2O_5-structured U_2O_5 is the most stable of those considered under ambient conditions. The observed δ-U_2O_5 structure is found to be second most stable and, surprisingly, given that is contains only octahedrally coordinated U is closely followed by R-Nb_2O_5. The bulk moduli of the most stable polymorphs are also very similar to U_3O_8, as would be expected given their close structural resemblance.

Hence, one could infer that the order of stability of U_2O_5 increases with the concentration of U^{5+} and oxygen content before reaching the U_3O_8 stoichiometry, which will stabilize U^{6+}, destabilizing the U_2O_5 phases. To this end it would be expected that uranium can crystallise with the Np_2O_5 structure, however it has not been observed experimentally. We suggest it is due to a combination of synthesis difficulties, as the composition is meta-stable with respect to U_3O_8, and the fact that the Np2O5 structure is destabilised with respect to the observed δ-U2O5 structure at the high temperatures and pressures more commonly used in many of the reported structural investigations of this composition from the 1960s. The stoichiometry is clearly worthy of synthetic investigation though as the Np_2O_5 structure is found to be a stable phase. The experimental challenge will be to develop lower temperature synthesis routes while calibrating the oxygen content extremely carefully.

Future simulation work will focus on using a more pragmatic approach to model fluorite-based U_2O_5 phases, potentially using the methodology set out in our previous studies of U_4O_9 [12] and U_3O_7 [13], in order to better understand the fluorite to layered transformation.

ASSOCIATED CONTENT

Supporting Information includes Density Functional Theory optimized uranium oxides at the U_2O_5 stoichiometry in the fractional format. The zone centre vibrational frequencies, the independent elastic constants, and thermodynamic properties are also presented. This material is available free of charge via the Internet at http://pubs.acs.org.

AUTHOR INFORMATION

Corresponding Author

* S.C.Parker@bath.ac.uk

ORCID

Marco Molinari: 0000-0001-7144-6075

Stephen C. Parker: 0000-0003-3804-0975

Funding Sources

Materials Chemistry Consortium funded by EPSRC (EP/L000202).

Notes

The authors declare no competing financial interest.

ACKNOWLEDGMENT

The authors thank the University of Bath for funding and AWE plc for their support and contribution. Computations were run on ARCHER through the Materials Chemistry Consortium funded by EPSRC (EP/L000202). We also made use of the HPC resources at the University of Bath and at the University of Huddersfield.

REFERENCES

(1) Hoekstra, H. R.; Siegel, S.; Gallagher, F. X. The Uranium-Oxygen System at High Pressure. *J. Inorg. Nucl. Chem.* **1970,** 32, 3237-3248.

(2) Allen, G. C.; Tempest, P. A. Ordered Defects in the Oxides of Uranium. *Proc. R. Soc. A: Mathem. Phys. & Eng. Sci.* **1986,** 406, 325-344.

(3) Brincat, N. A.; Parker, S. C.; Molinari, M.; Allen, G. C.; Storr, M. T. Density Functional Theory Investigation of the Layered Uranium Oxides U_3O_8 and U_2O_5. *Dalton Trans.* **2015,** 44, 2613-2622.

(4) Andersson, D. A.; Baldinozzi, G.; Desgranges, L.; Conradson, D. R.; Conradson, S. D. Density Functional Theory Calculations of UO_2 Oxidation: Evolution of UO_{2+X}, U_4O_{9-Y}, U_3O_7, and U_3O_8. *Inorg. Chem.* **2013,** 52, 2769-2778.

(5) Guéneau, C.; Baichi, M.; Labroche, D.; Chatillon, C.; Sundman, B. Thermodynamic Assessment of the Uranium–Oxygen System. *J. Nucl. Mater.* **2002,** 304, 161-175.

(6) McEachern, R. J.; Taylor, P. A Review of the Oxidation of Uranium Dioxide at Temperatures Below 400°C. *J. Nucl. Mater.* **1998,** 254, 87-121.

(7) Desgranges, L.; Baldinozzi, G.; Rousseau, G.; Niepce, J. C.; Calvarin, G. Neutron Diffraction Study of the in Situ Oxidation of UO_2. *Inorg. Chem.* **2009,** 48, 7585-7592.

(8) Leinders, G.; Delville, R.; Pakarinen, J.; Cardinaels, T.; Binnemans, K.; Verwerft, M. Assessment of the U_3O_7 Crystal Structure by X-Ray and Electron Diffraction. *Inorg. Chem.* **2016,** 55, 9923-9936.

(9) Kovba, L. M.; Komarevtseva, N. I.; Kuz'mitcheva, E. U. On the Crystal Structures of $U_{13}O_{34}$ and δ-U_2O_5. *Radiokhimiya* **1979,** 21, 754-757.

(10) Brincat, N. A.; Parker, S. C.; Molinari, M.; Allen, G. C.; Storr, M. T. Ab Initio Investigation of the UO_3 Polymorphs: Structural Properties and Thermodynamic Stability. *Inorg. Chem.* **2014,** 53, 12253-12264.

(11) Allen, G. C.; Holmes, N. R. A Mechanism for the UO_2 to α-U_3O_8 Phase Transformation. *J. Nucl. Mater.* **1995,** 223, 231-237.

(12) Brincat, N. A.; Molinari, M.; Parker, S. C.; Allen, G. C.; Storr, M. T. Computer Simulation of Defect Clusters in UO_2 and Their Dependence on Composition. *J. Nucl. Mater.* **2015,** 456, 329-333.

(13) Brincat, N. A.; Molinari, M.; Allen, G. C.; Storr, M. T.; Parker, S. C. Density Functional Theory Calculations of Defective UO_2 at U_3O_7 Stoichiometry. *J. Nucl. Mater.* **2015,** 467, 724-729.

(14) Pireaux, J. J.; Riga, J.; Thibaut, E.; Tenret-Noël, C.; Caudano, R.; Verbist, J. J. Shake-up Satellites in the X-Ray Photoelectron Spectra of Uranium Oxides and Fluorides. A Band Structure Scheme for Uranium Dioxide, UO_2. *Chem. Phys.* **1977,** 22, 113-120.

(15) Teterin, Y. A.; Teterin, A. Y. The Structure of the X-Ray Photoelectron Spectra of Light Actinide Compounds. *Uspekhi Khimii* **2004,** 73, 588-631.

(16) Kresse, G.; Hafner, J. Ab-Initio Molecular-Dynamics Simulation of the Liquid-Metal Amorphous-Semiconductor Transition in Germanium. *Phys. Rev. B* **1994,** 49, 14251-14269.

(17) Kresse, G.; Furthmuller, J. Efficient Iterative Schemes for Ab Initio Total-Energy Calculations Using a Plane-Wave Basis Set. *Phys. Rev. B* **1996,** 54, 11169-11186.

(18) Perdew, J. P.; Burke, K.; Ernzerhof, M. Generalized Gradient Approximation Made Simple. *Phys. Rev. Lett.* **1996,** 77, 3865-3868.

(19) Dudarev, S. L.; Botton, G. A.; Savrasov, S. Y.; Humphreys, C. J.; Sutton, A. P. Electron-Energy-Loss Spectra and the Structural Stability of Nickel Oxide: An LSDA+U Study. *Phys. Rev. B* **1998,** 57, 1505-1509.

(20) Anisimov, V. I.; Zaanen, J.; Andersen, O. K. Band Therory and Mott Insulators - Hubbard-U Instead of Stoner-I. *Phys. Rev. B* **1991,** 44, 943-954.

(21) Yamazaki, T.; Kotani, A. Systematic Analysis of 4f Core Photoemission Spectra in Actinide Oxides. *J. Phys. Soc. Jpn.* **1991,** 60, 49-52.

(22) Meredig, B.; Thompson, A.; Hansen, H. A.; Wolverton, C.; van de Walle, A. Method for Locating Low-Energy Solutions within DFT + U. *Phys. Rev. B* **2010,** 82, 195128.

(23) Wen, X.-D.; Martin, R. L.; Roy, L. E.; Scuseria, G. E.; Rudin, S. P.; Batista, E. R.; McCleskey, T. M.; Scott, B. L.; Bauer, E.; Joyce, J. J.; Durakiewicz, T. Effect of Spin-Orbit Coupling on the Actinide Dioxides AnO_2 (An=Th, Pa, U, Np, Pu, and Am): A Screened Hybrid Density Functional Study. *J. Chem. Phys.* **2012,** 137, 154707

(24) Flitcroft, J. M.; Molinari, M.; Brincat, N. A.; Storr, M. T.; Parker, S. C. Hydride Ion Formation in Stoichiometric UO_2. *Chem. Commun.* **2015,** 51, 16209-16212.

(25) Wen, X.-D.; Martin, R. L.; Scuseria, G. E.; Rudin, S. P.; Batista, E. R.; Burrell, A. K. Screened Hybrid and DFT + U Studies of the Structural, Electronic, and Optical Properties of U_3O_8. *J. Phys. Condens. Matter* **2013,** 25, 13122–13128.

(26) Molinari, M.; Tompsett, D. A.; Parker, S. C.; Azough, F.; Freer, R. Structural, Electronic and Thermoelectric Behaviour of $CaMnO_3$ and $CaMnO_{3-\delta}$. *J. Mater. Chem. A* **2014,** 2, 14109-14117.

(27) Forbes, T. Z.; Burns, P. C.; Skanthakumar, S.; Soderholm, L. Synthesis, Structure, and Magnetism of Np_2O_5. *J. Am. Chem. Soc.* **2007,** 129, 2760–2761.

(28) Gruehn, R. Eine Weitere Neue Modifikation Des Niobpentoxids. *J. Less Common Met.* **1966,** 11, 119-126.

(29) Zibrov, I. P.; Filonenko, V. P.; Werner, P. E.; Marinder, B. O.; Sundberg, M. A New High-Pressure Modification of Nb_2O_5. *J. Solid State Chem.* **1998,** 141, 205-211.

(30) Andersson, S. Crystal Structure of N-Nb_2O_5 Prepared in Presence of Small Amounts of LiF. *Z. Anorg. Allg. Chem.* **1967,** 351, 106-112.

(31) Zibrov, I. P.; Filonenko, V. P.; Sundberg, M.; Werner, P. E. Structures and Phase Transitions of B-Ta_2O_5 and Z-Ta_2O_5: Two High-Pressure Forms of Ta_2O_5. *Acta Crystallogr. Sect. B-Struct. Commun.* **2000,** 56, 659-665.

(32) Cocciantelli, J. M.; Gravereau, P.; Doumerc, J. P.; Pouchard, M.; Hagenmuller, P. On the Preparation and Characterization of a New Polymorph of V_2O_5. *J. Solid State Chem.* **1991,** 93, 497-502.

(33) Filonenko, V. P.; Sundberg, M.; Werner, P. E.; Zibrov, I. P. Structure of a High-Pressure Phase of Vanadium Pentoxide β-V_2O_5. *Acta Crystallogr. Sect. B-Struct. Commun.* **2004,** 60, 375-381.

(34) Shannon, R. D. Revised Effective Ionic-Radii and Systematic Studies of Interatomic Distances in Halides and Chalcogenides. *Acta Crystallogr. Sect. A* **1976,** 32, 751-767.

(35) Driscoll, R. J. P.; Wolverson, D.; Mitchels, J. M.; Skelton, J. M.; Parker, S. C.; Molinari, M.; Khan, I.; Geeson, D.; Allen, G. C. A Raman Spectroscopic Study of Uranyl Minerals from Cornwall, UK. *RSC Adv.* **2014,** 4, 59137-59149.

(36) Herzberg, G. Forbidden Transition in Diatomic Molecules: II. The Adsorption Bands of the Oxygen Molecule. *Can. J. Phys.* **1952,** 30, 185-210.

(37) Yeandel, S. R.; Molinari, M.; Parker, S. C. Nanostructuring Perovskite Oxides: The Impact of $SrTiO_3$ Nanocube 3D Self-Assembly on Thermal Conductivity. *RSC Adv.* **2016,** 6, 114069-114077.

(38) He, H.; Andersson, D. A.; Allred, D. D.; Rector, K. D. Determination of the Insulation Gap of Uranium Oxides by Spectroscopic Ellipsometry and Density Functional Theory. *J. Phys. Chem. C* **2013,** 117, 16540-16551.

For Table of Contents Only

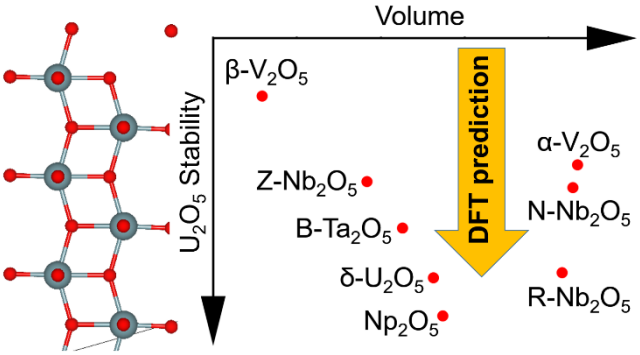

Density Functional Theory calculations were employed to predict layered structures of uranium oxide at U_2O_5 stoichiometry using known structures with the same composition. The structures are characterized in terms of relative stability and structural, elastic and electronic properties. U_2O_5 in the Np_2O_5 structure is predicted to be the most stable uranium pentoxide.